tecnia
revista de educação, ciência e tecnologia do IFG

OPEN ACCESS

Volume 11, Número 1, 2026

Effect of different mineral additions on colored self-compacting micro concrete produced with residual sand

Efeito de diferentes adições minerais em microconcretos autoadensáveis coloridos produzidos com areia residual

Efecto de diferentes adiciones minerales sobre el microhormigón autocompactante coloreado elaborado con arena residual

ANDRESSA DE ANDRADE TASSI[1]

EDGAR BACARJI[2]

OSWALDO CASCUDO MATOS[3]

RESUMO

O microconcreto autoadensável difere do concreto plástico tradicional porque elimina os agregados graúdos e apresenta alta fluidez e estabilidade no estado fresco. Sua utilização, aliada ao aproveitamento de resíduos, agrega valor técnico, econômico e ambiental. Além disso, amplia o espectro de aplicações do concreto Portland. O presente trabalho avaliou os efeitos da incorporação de diferentes adições minerais em microconcretos autoadensáveis coloridos, produzidos com areia artificial proveniente de britagem de rochas. Foram definidas três proporções de ligante: agregado, em massa, quais sejam: 1:3,0, 1:4,5 e 1: 5,5. Como adições, foram utilizados um pigmento inorgânico de coloração amarela e dois materiais cimentícios suplementares de natureza pozolânica: sílica ativa e nanossílica. Em seguida, foram avaliadas propriedades no estado fresco, como fluidez, viscosidade plástica e segregação. No estado endurecido, foram analisados as resistências à compressão, à tração e o módulo de elasticidade. As adições minerais implicam em alterações reológicas nas misturas, produzindo geralmente aumento da viscosidade e redução da segregação, além de se destacarem em termos de aumento da resistência mecânica. As misturas híbridas compostas por pigmento, sílica ativa e nanosílica, misturas quaternárias com cimento obtiveram os melhores resultados em termos de desempenho mecânico, apresentando sinergia significativa devido ao uso combinado desses materiais.

Palavras-chave: microconcreto autoadensável; areia artificial; pigmento; sílica ativa; nano-sílica.

ABSTRACT

Self-compacting micro concrete differs from traditional plastic concrete in that it eliminates coarse aggregate and has high fluidity and stability in the fresh state. Its use, combined with the use of waste, adds technical, economic, and environmental value. In addition, it expands the spectrum of applications of Portland concrete. The present work evaluated the effects of the incorporation of different mineral additions in colored self-compacting micro concrete, produced with artificial sand from rock crushing. Three binder: aggregate proportions (by mass) were used: 1:3.0, 1:4.5, and 1:5.5. As additions, a yellow-colored inorganic pigment and two supplementary cementitious materials of pozzolanic nature were used: silica fume and nanosilica. Then, properties were evaluated in the fresh state, such as fluidity, plastic visco-

1 Pontifícia Universidade Católica de Goiás (PUC Goiás). ORCID: https://orcid.org/0000-0003-2567-4100. Lattes: http://lattes.cnpq.br/1474526074064963. E-mail: andressatassi@hotmail.com.

2 Universidade Federal de Goiás (UFG). ORCID: https://orcid.org/0000-0003-2954-2260. Lattes: http://lattes.cnpq.br/2385473000869120. E-mail: edgar@ufg.br.

3 Universidade Federal de Goiás (UFG). ORCID: https://orcid.org/0000-0003-1879-6396. Lattes: http://lattes.cnpq.br/3336749062812376. E-mail: ocascudo@ufg.br.

sity, and segregation. In the hardened state, compressive, tensile strengths, and modulus of elasticity were analyzed. Mineral additions implied rheological changes in the mixtures, in general producing an increase in viscosity and a reduction in segregation, as well as being outstanding in terms of increased mechanical strength. The hybrid mixtures composed of pigment, silica fume, and nanosilica, quaternary mixtures with cement, obtained the best results in terms of mechanical performance, showing significant synergy due to the combined use of these materials.

Keywords: self-compacting micro concrete; crushing sand; pigment; silica fume; nanosilica.

RESUMEN

El micro hormigón autocompactante se diferencia del hormigón plástico tradicional porque elimina los áridos gruesos y presenta una alta fluidez y estabilidad en estado fresco. Su utilización, combinada con el aprovechamiento de residuos, añade valor técnico, económico y ambiental. Además, amplía el espectro de aplicaciones del hormigón Portland. Este estudio evaluó los efectos de incorporar diferentes adiciones minerales en micro hormigones autocompactantes coloreados producidos con arena artificial a partir de rocas trituradas. En el estudio se utilizaron tres proporciones de aglomerante: agregado (por masa): 1:3.0, 1:4.5 y 1:5.5. Como añadidos se utilizaron un pigmento inorgánico de color amarillo y dos materiales cementantes suplementarios de naturaleza puzolánica: humo de sílice y nanosílice. Luego, se evaluaron propiedades en estado fresco, como la fluidez, la viscosidad plástica y la segregación. En estado endurecido se analizaron las resistencias a la compresión y a la tracción, así como el módulo de elasticidad. Las adiciones minerales implican cambios reológicos en las mezclas, produciendo generalmente un aumento de la viscosidad y una reducción de la segregación, además de destacarse en términos de aumento de la resistencia mecánica. Las mezclas híbridas compuestas de pigmento, sílice activa y nano-sílice, y mezclas cuaternarias con cemento, obtuvieron los mejores resultados en términos de desempeño mecánico, presentando una sinergia significativa debido al uso combinado de estos materiales.

Palabras clave: micro hormigón autocompactante; arena triturada; pigmento. humo de sílice; nano-sílice.

1 INTRODUCTION

With the developments in society, mainly in the construction industry, there has been a huge growth in the demand for sand in many countries (Cai *et al*., 2021). The extraction of natural sand from riverbeds is responsible for adverse environmental impacts, since it causes both the removal of vegetation cover and the alteration of the watercourse, in addition to other harmful environmental effects (Barbosa; Coura, Mendes, 2008). On the other hand, during the rock fragmentation process up to the required dimensions, a certain percentage of the total material is produced with smaller dimensions than those corresponding to the range of the coarse aggregate. Such a fraction, called artificial sand in some Brazilian regions or simply crushing sand, is considered a residue of the rocks' comminution process, being stored in piles in quarry yards. Considering that crushing sand is a residue that generates a significant environmental liability, considering that the deposits of natural sand are increasingly scarce, with its exploitation causing the degradation of the environment, frequent studies have been conducted on mortars and concrete in which the replacement of natural sand by crushing sand is promoted (Vijayalakshmi; Sekar; Prabhu, 2013; Ingalkar; Harle, 2017; Tokarski; Matoski; Cechin; Weber, 2018; Nguyen; Nguyen; Lam, 2022). The replacement of this

traditional material with residual material demonstrates the potential of the artificial sand and the feasibility of its use, contributing to ecological preservation, and becoming an economically attractive and environmentally more appropriate alternative (Mundra, *et al*., 2016).

With the advancement of the civil construction industry, new needs have emerged in this professional engineering market. Although conventional concrete with plastic consistency, traditionally made with natural sand and crushed stone, already meets a wide range of market demands, there are increasing alternatives in terms of special concretes (such as micro concrete, for example) with specific characteristics to meet design and construction requirements, thus contributing to a better overall performance of the concrete structural system. Micro concrete differs from conventional standard concrete by eliminating the coarse aggregate, thus allowing the production of slender elements, with potential emphasis on prefabricated components. This special concrete can also be applied in smaller constructions and in lightweight precast components used in traditional construction, often with lower structural responsibility, and even in non-structural applications, such as the manufacture of partition components or prefabricated panels. An additional application of micro concrete is in the field of structural repair and strengthening (KadamSIngh, Li, 2014; Jonbi *et al*., 2018). The maximum nominal size of aggregates for micro concrete may vary according to the intended application or research purpose. However, since the total aggregates have a greater specific surface area, the volume of paste required to coat the aggregates is larger (compared to conventional plastic concretes), which generally leads to more plastic mixtures with greater workability (Felekoğlu, 2007).

Generally, micro concrete is composed of Portland cement, fine aggregates duly characterized, certain content of gravel (fraction below the zone d/D = 4.75/12.5 but above the sand) and admixtures that control the behavior of the material in the plastic state, due to the low water/cement ratio and the amount of fine materials (Silva; Bacarji; Cascudo, 2019; Campos, 2017). If, among several rheological requirements, the goal is to design a material that exhibits high fluidity combined with a self-compacting profile without segregation, it evolves into a self-compacting micro concrete (Tutikian, Dal Molin; Cremonini, 2008). One of the main challenges in producing these concretes lies in controlling their properties, especially regarding water bleeding and aggregate segregation. One possible way to control these phenomena is through the addition of fine materials to the mixture, such as silica fume and nanosilica. The surface exposure of these ultrafine particles, at the micro and nanoscale, provides surface area for interaction with the mixing water molecules (enhancing the physical adsorption of polar water molecules onto the particle surface), which improves cohesion in the plastic state, modifies viscosity, and reduces segregation and bleeding (Oliveira; Oliveira; Cascudo, 2019). In this sense, the proper selection of materials and the correct proportioning of the mix constituents are essential to achieve an adequate rheological composition of the concrete.

In the hardened state, the interactions of the mineral additions in the cementitious matrix modify the microstructural characteristics and, consequently, the properties of the concrete and the overall performance of the structural system under service conditions. The influence of silica fume on the internal structure of concrete is well known (Oliveira; Cascudo, 2018; Cascudo *et al*., 2020) and occurs based on two main effects: a chemical effect, of pozzolanic nature, and a physical effect, the so-called filler effect. Pozzolanic reactions occur due to the chemical interaction between amorphous silica (SiO_2), the main constituent of silica fume, and calcium hydroxide [$Ca(OH)_2$] produced by cement hydration (specifically from the reactions of the two types of calcium silicate in anhydrous cement – C_3S and βC_2S). This interaction results in additional formation of calcium silicate hydrate (C–S–H), a compound that positively alters the pore structure, making the cement paste denser, more homogeneous, and more compact. The filler effect occurs due to the small size of the silica fume particles, which fill the voids in the concrete, improving particle packing and cohesion, and acting as nucleation sites (Oertel *et al*., 2014; Isaia; Gastaldini; Moraes, 2003). The addition of silica fume leads to a more homogeneous distribution of hydration products, making the concrete less permeable and, consequently, more durable. Moreover, the reduction of voids and the improvement of the microstructure increase the compressive strength (Rezaei-Ochbelagh; Azimkhani; Mosavinejad, 2012). In general, partial replacement of cement with silica fume in the range of 8% to 12% (by mass) produces very satisfactory results in terms of microstructure and mechanical strength improvement (Wongkeo Thongsanitgarn; Chaipanich, 2012). It is important to note, however, that the optimal amount of silica fume depends on its characteristics as a supplementary cementitious material—particularly its fineness and pozzolanic activity—as well as the concrete mix design and property requirements. These variables may justify contents slightly higher than 12% or lower than 8%, but this range is commonly used.

Nanometer-sized silica particles are called nanosilica. These nanoparticles can accelerate cement hydration by nucleation, due to their high fineness. Additionally, their high reactivity and, therefore, greater capacity for pozzolanic interaction with calcium hydroxide promote faster kinetics in the formation of calcium silicate hydrate (C–S–H), making this effect more pronounced than that of silica fume alone. Nanosilica particles consume calcium hydroxide crystals (CH), reduce their orientation and size, and improve the paste–aggregate interface. As a result, greater densification of the cement matrix is achieved and, consequently, higher strength and durability of pastes, mortars, or concretes (Madandoust *et al*., 2015). Usually, the combined action of silica fume, and nanosilica generates the most significant results in improving the microstructure of concrete, since it produces important synergistic effects (Oliveira; Oliveira; Cascudo, 2019).

Among the additions used for concretes with special characteristics, pigments are employed for the permanent coloring of mortars, concrete pavers, concrete tiles, and precast concrete products (Lee; Lee; Yu, 2003). It is known that colored concrete can be obtained using additions such as marble powder combined with inorganic pigments. The addition of pigments can increase or decrease mechanical properties and durability, depending on their proportions (Uysal, 2018). It is also necessary to consider the physical properties of pigments in cement composites, since their addition changes the consistency of the mixture, generally modifying the rheological behavior of the concrete. The variations in specific surface area among pigments depend on particle size and shape. The yellow pigment has acicular (needle-shaped) particles, unlike other pigments such as green and red, whose particles have more spherical geometries (Jang; Kang; So, 2014).

Thus, although there is already research on the effects of the mentioned materials on the properties of self-compacting concrete, there is a lack of studies on micro concrete, especially those made exclusively with crushed sand. There is also a lack of studies evaluating the combined effects of these additions and verifying the synergy of these materials when they present different granulometries and effects. These are the gaps that the present research intends to address. The results presented here contribute to the current state of the art, as they apply known methodologies to a material such as micro concrete that can replace conventional concrete in specific situations, such as those involving a high concentration of reinforcing bars.

The decision to use yellow pigment was based on its frequent application in colored concrete, thus expanding the range of potential uses of the material within the field of special pigmented concretes. The other additions (silica fume and nanosilica) were selected because they are pozzolans known to effectively modify the microstructure of concrete and, additionally, to influence rheological behavior, given the different orders of magnitude of their particle sizes, with dimensions in the micro- and nanoscale. Therefore, the importance of this study lies in the fact that the behavior of self-compacting micro concrete with the proposed materials is still not well known by the academic and technical community. This study is also of greater relevance because it considers three different proportions between binders and aggregates, covering distinct possibilities of material application.

The general objective of this work was to evaluate the effects of yellow pigment, silica fume, and nanosilica on the properties of self-compacting micro concrete, produced with crushed sand in three proportions between binders and aggregates. The properties in the fresh and hardened state were evaluated. Specifically, the individual effects of the yellow pigment and silica fume were analyzed, as well as the combined effects of pigment and silica fume, and of pigment, silica fume, and nanosilica. As a last objective, the paper proposed to discuss a technically and environmentally

correct destination for the crushed sand, which remains in companies' yards. Among the properties evaluated to meet these objectives, this study considered the basic requirements for self-compacting micro concrete in the fresh state, as well as the mechanical and elastic properties of the hardened concrete (compressive and tensile strength and modulus of elasticity).

The hypotheses were that the combined effects result in improved material properties compared to the individual effects, and that such effects differ depending on the proportions adopted between binders and aggregates.

2 MATERIALS AND METHODS

2.1 Materials constituting the mixtures

Cement

The cement used to produce the mixtures was white Portland cement - CPB-40, with a Blaine specific area equal to 515.7 m^2/kg and a specific mass of 3,110 kg/m3. The chemical composition results of the cement used are shown in Table 1.

Determined Properties		Results (%)	Limits of NBR 16697 (ABNT, 2018) (%)
Chemical Composition	Loss to fire	2.85	< 12.0
	Insoluble residue	0.31	< 3.5
	Sulfur trioxide (SO3)	4.16	< 4.5
	Magnesium oxide (MgO)	0.72	< 6.50
	Silicon dioxide (SiO2)	21.48	-----
	Iron oxide (Fe2O3)	0.2	-----
	Aluminum oxide (Al2O3)	4.6	-----
	Calcium oxide (CaO)	65.18	-----
	Free calcium oxide (CaO)	2.23	-----
Total Alkalis	Sodium oxide (Na2O)	0.13	-----
	Potassium oxide (K2O)	0.14	-----
	Alkaline equivalent	0.22	-----

Table 1 – Chemical composition of CPB-40 Portland cement used in the research.
Source: Furnas Centrais Elétricas (2024).

Supplementary additions

As additions, silica fume and suspension nanosilica (stabilized nanosilica, already contained in superplasticizer "A") were used. The silica fume presented a specific mass equal to 2,280 kg/m^3 and a diameter d50 of 0.42 µm. The nanosilica presented a diameter varying between 0.01 µm and 1.0 µm according to the manufacturer's specification.

Yellow pigment

The pigment used was iron oxide, whose chemical characterization is shown in Table 2.

Chemical Constituents (%)	Determined Properties		
	Specific Mass (g/cm^3)		3.99
	Loss to fire (%)		11.53
	Insoluble residue (%)		90.4
	Sulfur trioxide (SO3) (%)		0.78
	Magnesium oxide (MgO) (%)		1.15
	Silicon dioxide (SiO2) (%)		0.23
	Iron oxide (Fe2O3) (%)		86.39
	Aluminum oxide (Al2O3) (%)		0.20
	Calcium oxide (CaO) (%)		0.11
	Alkalis Totals	Sodium oxide (Na2O) (%)	0.14
		Potassium oxide (K2O) (%)	0.02
		Alkaline equivalent (%)	0.04

Table 2 – Chemical composition of the pigment (iron oxide) used in the research.
Source: Furnas Centrais Elétricas (2024).

The Scanning Electron Microscopy (SEM) and Transmission ElectronElectron Microscopy images of the pigment are given in Figure 1 and Figure 2, respectively.

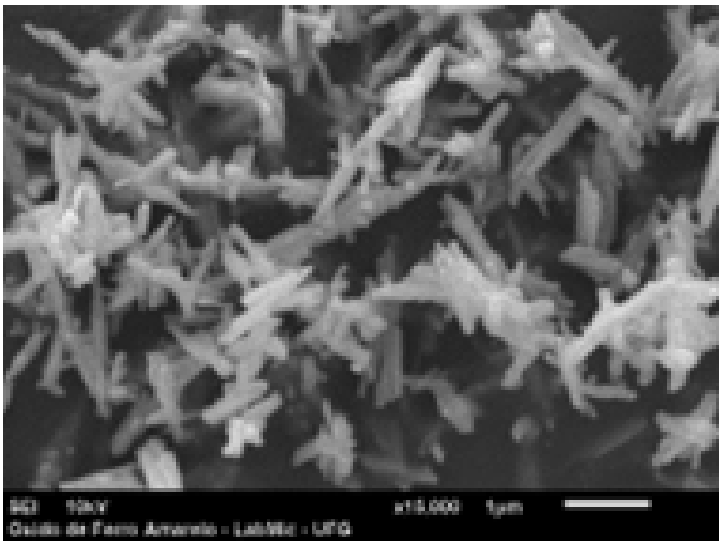

Figure 1 – Microscopic image obtained by scanning electron microscopy (SEM) - via secondary electron detector - of iron oxide used as a yellow pigment in the composition of microconcretes.
Source: LabMic – UFG (2024).

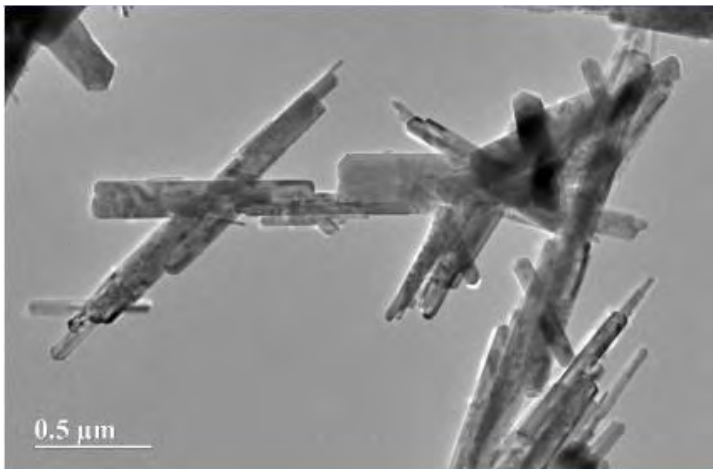

Figure 2 – Microscopic image obtained by transmission electron microscopy (TEM) of a sample of iron oxide used as a yellow pigment in the composition of microconcretes. The irregular and elongated shape of the magnified pigment particles can be seen.
Source: LabMic – UFG (2024).

Aggregates

As aggregates, artificial sand from granitic rock crushing was used, with a specific mass equal to 2,650 kg/m^3, fineness modulus (FM) equal to 3.16, characteristic maximum dimension (Dmax) equal to 4.75 mm, and fine material content (passing through the 0.15 mm sieve) of 9.0%. The SEM of this fine material content is given in Figure 3.

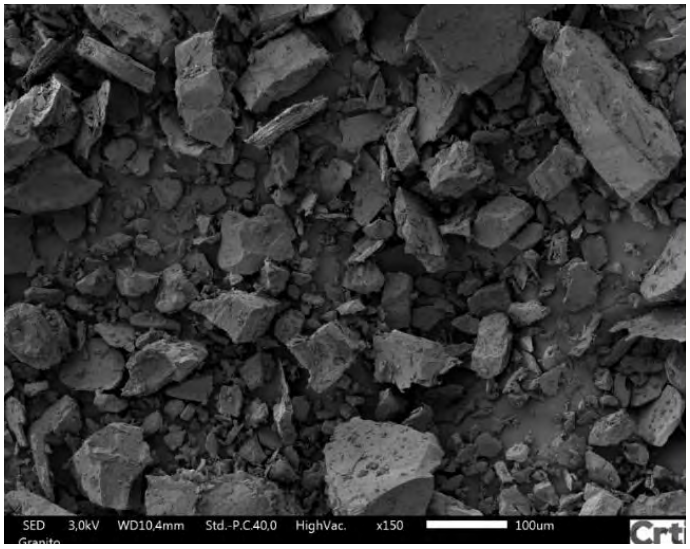

Figure 3 – A slightly magnified microscopic image of the fines present in the aggregate used (artificial sand from crushed granite rock), obtained by scanning electron microscopy (SEM) using a secondary electron detector, shows the particles' high degree of angularity as well as their high variability in size and shape.
Source: Crti – UFG (2023).

The granulometric distributions of the silica fume, pigment, cement, and sand are summarized in the graph in Figure 4.

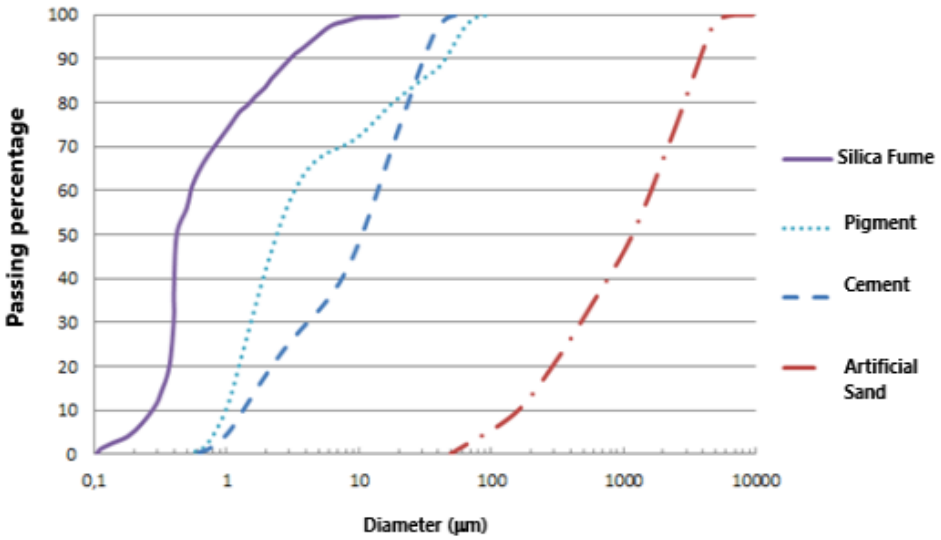

Figure 4 – Granulometric curves of all materials constituting the studied microconcretes (silica fume, pigment, Portland cement, and artificial sand).
Source: Author's personal catalogue (2025).

Two types of superplasticizer additives were used, both based on polycarboxylates. One was the vehicle itself containing dispersed nanosilica (SPP A), and the other was a conventional superplasticizer, intended exclusively for use in concrete (SPP B). Both superplasticizers were added in relation to the binders (cement or cement and silica fume, when applicable).

2.2 Studied mixtures – concrete mix proportions, production,x, and curing of specimens

After the characterization of the materials, the quartering of the artificial sand was performed to ensure homogeneity and uniformity in terms of the granulometry and moisture content of this material. Next, the mixtures were prepared with the following binder-to-aggregate ratios (by mass): 1:3.0, 1:4.5, and 1:5.5, initially without the incorporation of additions, thus representing the reference mixtures (R).

In sequence, the other mixtures were produced with the addition of pigment and silica fume, separately. The incorporation of the colored pigment into the micro concrete was performed by adding 2% relative to the binder mass (mixture P), while the silica fume was incorporated as a partial replacement of 10% of the binder mass (mixture S). The 2% pigment content relative to the binder mass was chosen based on the manufacturer's recommendation, which suggests a dosage between 1% and 2%. The upper limit was selected to enhance the color intensity of the micro concrete, even in mixtures with a low cement content. For silica fume, a 10% content represents the lower limit

of the commonly recommended range (10–20%) and was intentionally selected to evaluate whether even a minimal addition would be sufficient to improve the properties of the microconcretes. The mixtures with combined additions were as follows: pigment with silica fume (PS mixture) and pigment with silica fume and nanosilica (PSNs mixture). The nanosilica used was dispersed in superplasticizer A; therefore, this superplasticizer was applied only in mixtures containing nanosilica. In the other mixtures, without nanosilica, superplasticizer B was always used. Depending on the binder-to-aggregate ratio, the mixtures were designated as shown in Table 3. For the 1:3.0 ratio, the reference mixture was identified as 130R, and so on successively.

bin:aggr	Mixtures				
	Reference	2% Pigment	10% Silica	2% Pig.+10% Sil.	2% Pig.+10% Sil.+ Ns
1:3,0	130R	130P	130S	130PS	130PSNs
1:4,5	145R	145P	145S	145PS	145PSNs
1:5,5	155R	155P	155S	155PS	155PSNs

Table 3 – Identification of mixtures
Source: Author's personal catalogue (2025).

The dosage of the reference mixtures, once established in the unitary binder-to-aggregate proportion, consisted of determining the water-to-binder ratio (w/b) and the superplasticizer content to obtain acceptable fresh-state properties: a spread above 550 mm and segregation below 20%. The proportions of the studied mixtures, along with the determined SPP and water-to-binder ratios, are presented in Table 4. Table 5 shows the material consumption per cubic meter of concrete.

Mixtures	Cement	Sand	Pigment	Silica Fume	SPP A	SPP B	w/bin
130R	1.0	3.0	-	-	-	0.006	0.5
130P	1.0		0.02	-	-	0.006	
130S	0.9		-	0.1	-	0.012	
130PS	0.9		0.02	0.1	-	0.012	
130PSNs	0.9		0.02	0.1	0.015	-	

145R	1.0	4.5	-	-	-	0.008	0.7
145P	1.0		0.02	-	-	0.010	
145S	0.9		-	0.1	-	0.012	
145PS	0.9		0.02	0.1	-	0.012	
145PSNs	0.9		0.02	0.1	0.015	-	
155R	1	5.5	-	-	-	0.008	0.92
155P	1		0.02	-	-	0.008	
155S	0.9		---	0.1	-	0.010	
155PS	0.9		0.02	0.1	-	0.010	
155PSNs	0.9		0.02	0.1	0.014	-	

Table 4 – Unit proportion (in mass) and w/bin relations of the mixtures
Source: Author's personal catalogue (2025).

Mixtures	Cement	Sand	Pigment	Silica Fume	SPP A	SPP B	Water
130R	438.6	1,315.8	-	-	-	2.63	219.3
130P	470.1	1,410.3	9.4	-	-	2.82	235.1
130S	448.7	1,495.5	-	49.8	-	5.98	249.3
130PS	447.0	1,490.1	9.9	49.7	-	5.96	248.4
130PSNs	416.6	1,388.7	9.3	46.3	6.95	-	231.5
145R	316,2	1,422,9	-	-	-	2.53	221.3
145P	334.2	1,503.9	6.7	-	-	3.34	233.9
145S	305.6	1,528.2	-	34.0	-	4.08	237.7
145PS	304.8	1,523.7	6.8	33.8	-	4.06	237.0
145PSNs	288.5	1,442.3	6.4	32.0	4.81	-	224.4
155R	262.9	1,446.0	-	-	-	2.10	241.9
155P	263.5	1,449.3	5.3	-	-	2.11	242.5
155S	247.4	1,512.0	-	27.5	-	2.75	252.9
155PS	244.4	1,493.3	5.4	27.1	-	2.72	249.8
155PSNs	245.2	1,498.2	5.5	27.2	3.81	-	250.6

Table 5 – Consumption of materials per m^3 of concrete (kg)
Source: Author's personal catalogue (2025).

To evaluate the properties of the self-compacting micro concrete in the fresh state, slump-flow, T500, V-funnel, and segregation column tests were performed. These tests were conducted according to the Brazilian Standards NBR 15823-2 (ABNT, 2017), NBR 15823-5 (ABNT, 2017), and NBR 15823-6 (ABNT, 2017), respectively. The Visual Stability Index (VSI) was determined by analyzing the micro concrete immediately after the end of flow. The distribution of aggregates within the mixture, the distribution of the mortar fraction along the perimeter, and the occurrence of bleeding were observed and photographically recorded. According to the aforementioned standards, the visual stability of self-compacting concrete is classified as follows: VSI0 corresponds to highly stable concrete, showing no signs of segregation or bleeding; VSI1 to stable concrete, with no segregation but slight bleeding; VSI2 to unstable concrete, characterized by a small paste halo (≤10 mm) or aggregate segregation at the center; and VSI3 to highly unstable concrete, where segregation is clearly evident, either by the concentration of aggregates at the center or by a large paste halo (>10 mm).

Considering that the potential application of the material in this research is the same as that of self-compacting concretes, no adaptations were made regarding the tests in the fresh state, except for the sieve used in the segregation column test, in which a 2.36 mm sieve was employed. For the T500 tests, all procedures were filmed, and the start and end times of the flow were recorded to minimize measurement inaccuracies. To evaluate the mechanical properties, compressive strength, modulus of elasticity, and tensile strength by diametral compression weretested at 28 days. The tests followed the requirements of NBR 5739 (ABNT, 2018), NBR 8522-1 (ABNT, 2021), and NBR 7222 (ABNT, 2011), respectively. For a better interpretation of the results, the values obtained for the mechanical properties were subjected to analysis of variance (Anova) using SISVAR software (Ferreira, 2019). In the Anova, Tukey's test was applied at a 95% confidence level.

The mixtures were prepared without using a specific mix design method for self-compacting concrete. This was due to the absence of coarse aggregate and the high fines content in the sand (as shown in its characterization), which together ensured good stability of the mixtures. Consequently, the dosing process was limited to adjusting the superplasticizer content after the water-to-binder ratio had been established.

3 RESULTS AND DISCUSSIONS

3.1 Results in the fresh state

The properties evaluated were the fluidity of the mixtures (measured by the Abram's cone spreading), the apparent plastic viscosity (measured by the T500 and V-funnel tests), and the segre-

gation resistance (measured by the segregation column test). These results are presented in Table 6. Figure 5 illustrates Abram's cone spreading of the mixtures, and the observed exudation aspects are shown in Figure 6.

Mixture	Entrained Air (%)	Density (kg/m³)	Slump-flow (mm)	T500 (s)	V -Funnel (s)	Segregation (%)
130R	2.5	1,973.68	750	0.79	2.58	-0.68
130P	2.5	2,125.00	800	0.31	2.89	9.88
130S	2.4	2,243.42	780	0.97	3.30	1.35
130PS	1.5	2,245.12	795	0.27	3.48	1.25
130PSNs	2.5	2,092.11	760	1.32	3.75	1.45
145R	3.7	1,960.53	565	1.74	2.59	10.69
145P	3.3	2,078.95	635	1.27	3.38	-6.82
145S	3.2	2,105.26	595	1.75	2.66	-2.01
145PS	4.8	2,106.23	615	1.56	2.35	-1.50
145PSNs	5.5	1993.42	555	2.49	3.19	0.51
155R	3.0	1,950.58	570	1.56	2.13	10.90
155P	3.5	1,960.53	595	0.31	1.70	8.30
155S	3.4	2,039.47	560	2.02	2.45	9.64
155PS	5.8	2,019.74	550	1.22	2.04	6.75
155PSNs	7.2	2,026.32	555	1.66	2.66	4.80

Table 6 – Results of micro concrete properties evaluated in the fresh state.
Source: Author's personal catalogue (2025).

Figure 5a – Abram's cone spreading of R, P, S mixtures.
Source: Author's personal catalogue (2025).

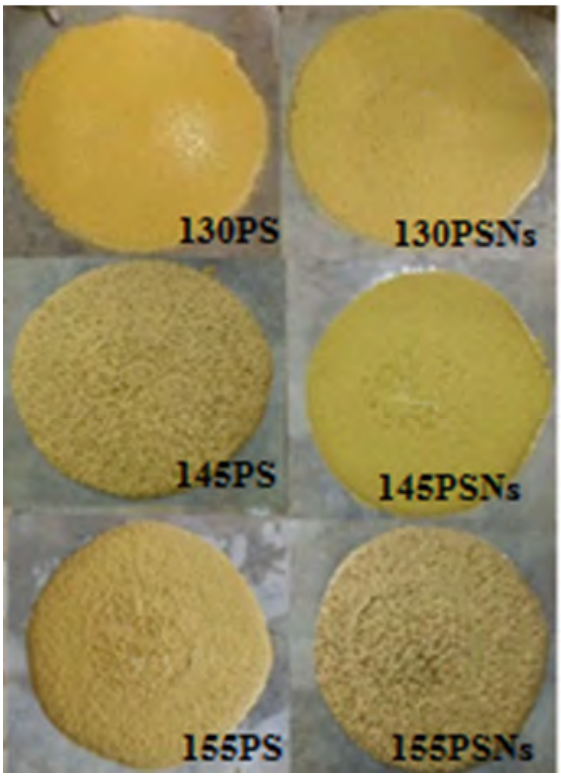

Figure 5b – Abram's cone spreading of PS and PSNs mixtures.
Source: Author's personal catalogue (2025).

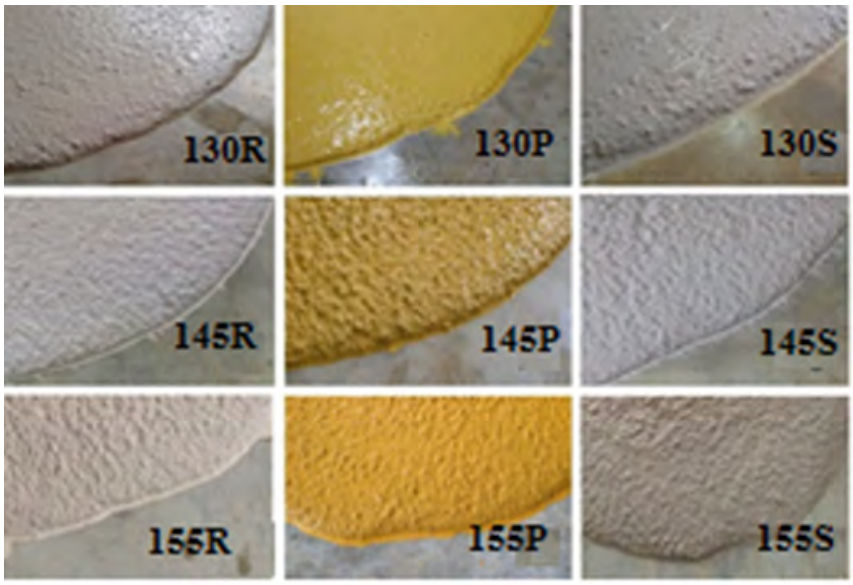

Figure 6a – Aspects of exudation of R, P, S mixtures.
Source: Author's personal catalogue (2025).

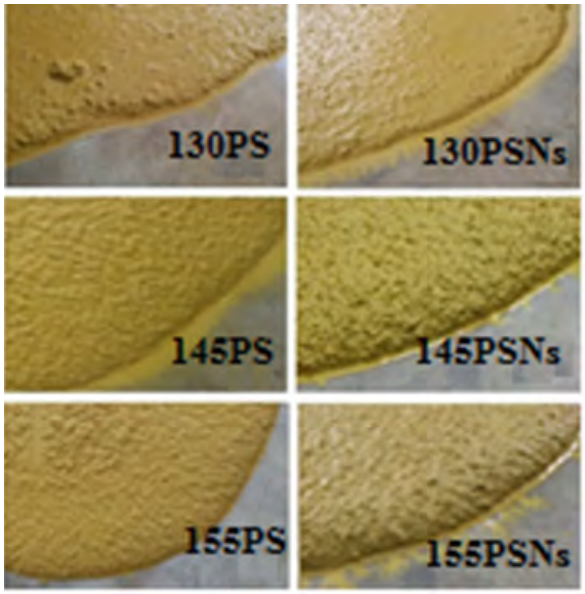

Figure 6b – Figure 6b – Aspects of exudation of PS and PSNs mixtures.
Source: Author's personal catalogue (2025).

3.2 VISUAL STABILITY INDEX

Analyzing the images in Figures 5 and 6, the following classifications according to NBR 15823-1 (ABNT, 2017) can be observed for the Visual Stability Index (VSI): VSI 0: mixtures 130R and 145P. VSI 1: mixtures 130P to 145R and 145S to 145PSNs. VSI 2: mixtures 155R to 155PSNs. These results are

relevant because they show, in general, that as the mixture composition shifts from a proportion richer in fines to a poorer one, the stability decreases, leading to segregation and bleeding.

3.2.1 Slump-flow

Comparing Abram's cone spreading of the mixtures with pigment addition (130P, 145P, and 155P) to the reference mixtures (130R, 145R, and 155R) in Table 5, an increase in fluidity was observed for all mixtures containing pigment. It was noted that for mixtures 130P and 155P, the superplasticizer contents did not vary in relation to the corresponding reference mixtures. It was also observed that the mixtures with pigment exhibited higher density. This indicates that the pigment incorporation, considering the order of magnitude of its particle dimensions shown in Figures 1, 2, and 4, resulted in improved particle packing. This condition, combined with a probable reduction in friction between aggregate particles, enhanced the fluidity of these mixtures. Such behavior was only possible because the paste volume was sufficient to reduce internal friction among aggregate particles, thus exerting a "lubricating" effect even when the specific surface area of the grains increased (with the incorporation of pigments), as a result of a particulate system that remained well dispersed throughout the rheological analyses.

For the mixtures containing silica fume, the increase in Abram's cone spreading (in mixtures 130S and 145S) was certainly due to the higher dosage of the superplasticizer additive, which was necessary to maintain the desired level of fluidity. This adjustment was required because the incorporation of finer silica fume particles, as shown in Figure 4, increased the specific surface area of the binder. In the case of mixtures with pigment, silica fume, and nanosilica, the water demand to achieve the same level of fluidity naturally increased due to the significant rise in the amount of fine particles in the system (i.e., a larger specific surface area). With the water content kept constant relative to the reference mixtures, adjustments were made by increasing the superplasticizer dosage, as presented in Table 4. Despite this, an increase in fluidity was observed only for the richest composition—with the highest binder content (130PSNs)—and even then, the improvement was very modest. The fluidity was already lower for the 145PSNs and 155PSNs mixtures than their respective reference mixtures. This can be attributed to the fact that these more complex systems (containing silica fume and nanosilica) promote greater cohesion in the fresh state. Furthermore, the fluidizing capacity of the additive decreases in mixtures with lower cement or binder content, as observed in mixtures 145PSNs and 155PSNs. The partial loss of superplasticizer effectiveness in more cohesive systems explains the reduction in fluidity observed in mixtures containing pigment, silica fume, and nanosilica. On a smaller scale, this reasoning also applies to mixtures containing only silica fume or

pigment and silica fume. In the less binder-rich compositions (155S and 155PS), the mixtures exhibited lower fluidity than the reference mixture (155R). In contrast, in the richer compositions (130S, 130PS, 145S, and 145PS), fluidity was consistently higher than in their respective reference mixtures.

Regarding the spreading results, it was observed that all mixtures with the 1:3.0 ratio, except for mixture 130R, were classified as SF3 (spreading between 760 mm and 850 mm) according to ABNT NBR 15823-1 (2017), which is suitable for structures with high reinforcement density or complex architectural geometries. Mixture 130R was classified as SF2 (spreading between 660 mm and 750 mm), applicable to most conventional structural applications. For the 1:4.5 and 1:5.5 ratios, all mixtures fell within the SF1 classification (spreading between 550 mm and 650 mm), which corresponds to applications in unreinforced structures or those with low reinforcement ratios, where a short horizontal flow distance of the self-compacting concrete is sufficient.

3.2.2 T500 Test

Regarding the apparent plastic viscosity under free flow, measured by the T500 test, it was found that the addition of pigment (mixtures 130P, 145P, and 155P) resulted in a significant reduction in viscosity compared with the reference mixtures (130R, 145R, and 155R). These reductions were 60.8%, 27.0%, and 80.1%, respectively. It was also observed that the T500 for mixture 130R was low, that is, well below 2 s. In general, for the mixtures with pigment, the reduction in viscosity explained the increase in fluidity observed in the previous subsection. For the mixtures with silica fume (130S and 155S), viscosity increased in relation to the corresponding reference mixtures, even with the increase in superplasticizer content. The observed increases were 22.8% and 29.5%, respectively. In the case of mixture 145S, the viscosity was practically the same as that of its reference mixture, 145R, since the superplasticizer content increased from 0.8% to 1.2%. This increase in viscosity indicated greater cohesion, a result of the high specific surface area of the silica fume, as already noted in the previous subsection. The addition of 2% pigment (mixtures 130PS, 145PS, and 155PS) to the mixtures containing silica fume (130S, 145S, and 155S) reduced viscosity, similarly to what occurred in mixtures 130P, 145P, and 155P. The observed reductions were 72.2%, 10.9%, and 39.6%, respectively. When nanosilica was incorporated into the mixtures with pigment and silica fume (130PSNs, 145PSNs, and 155PSNs), viscosity increased again in relation to mixtures 130PS, 145PS, and 155PS, by 388.9%, 59.6%, and 36.1%, respectively. Overall, mixtures that included silica fume or silica fume combined with nanosilica, with little interference from the pigment, exhibited higher apparent plastic viscosity, which is consistent with the greater cohesion in the plastic state observed in these compositions. In contrast, the incorporation of pigment alone reduced viscosity.

Considering ABNT NBR 15823-1 (2017), all mixtures, except for mixtures 145PSNs and 155S, were classified as VS1, that is, T500 ≤ 2 s. The remaining mixtures were classified as VS2, with T500 > 2 s.

3.2.3 V-Funnel test

Regarding the apparent plastic viscosity under confined flow (V-funnel test), some mixtures behaved differently compared with the free flow condition (T500). The mixtures that showed this behavior were 130P, 130PS, and 145P. In these cases, an increase in viscosity under confined flow was observed with the addition of the respective fines. It was also observed that for the 1:5.5 ratio, which is poorer in terms of binder content, all mixtures behaved similarly under both free flow and confined flow conditions. For a more in-depth discussion of these observations, rheological studies would be required, using a rheometer to determine the plastic viscosity and yield stress of the mixtures. In any case, a general tendency toward increased viscosity of particulate systems was observed as finer phases were added (for example, when pigment was incorporated) or when fine particles were partially replaced by even finer particles (through the incorporation of silica fume or silica fume and nanosilica). This behavior was attributed to the overall increase in the specific surface area of these particulate systems, which was clearly evident in the analysis of the apparent plastic viscosity under confined flow (V-funnel test). As the surface area of the systems increased, the available surfaces for water adsorption also increased. Water molecules, being polar, tended to interact with these surfaces, thereby reducing the amount of free water available (Cascudo, 2017). Consequently, water remained more strongly retained within the fresh mixture due to surface charge effects associated with the physical adsorption mechanism, contributing to greater water retention (Mehta & Monteiro, 2014). The practical effect was an increase in mixture cohesion in the plastic state, generally accompanied by higher viscosity (accentuated by the higher fines content), as well as significant reductions in segregation and water exudation.

For the aspect of apparent plastic viscosity under confined flow (V-funnel), according to NBR 15823-1 (ABNT, 2017), all mixtures were classified as VF1, that is, V-funnel < 9 s. Considering the requirements of the aforementioned Standard for both plastic viscosity results (under free and confined flow), mixtures 145PSNs and 155S could be applied in most current cases, while the others would be suitable for structures with high reinforcement density or complex architectural forms.

3.2.4 Segregation column

Regarding segregation, measured by the Column test, Table 6 shows the good stability of the reference mixture 130R, which exhibited no segregation. The homogeneous appearance of this

micro concrete can also be verified in Figures 5 and 6. One factor that influenced this behavior was the presence of cement fines, since this is a rich mixture (in cement), with a 1:3.0 (cement: aggregate) ratio. As the amount of fines decreased, this behavior was not maintained in mixtures 145R and 155R, which presented segregation levels of 10.69% and 10.90%, respectively. In Figure 5a, an accumulation of sand can be seen at the center—especially for mixture 155R—as well as the presence of exuded free water along the edges (Figure 6a), both effects resulting from mixture segregation. Thus, the 9% fines content in the sand, as shown in its characterization, together with the grain shape illustrated in Figure 3, was not sufficient to maintain the stability of mixtures 145R and 155R compared with mixture 130R.

When pigment was added to mixture 130P, segregation increased to 9.88%. In this case, the pigment reduced the already low plastic viscosity, as discussed in item 3.1.2, thereby increasing segregation. However, when analyzing Figure 5a, the perception of segregation was not so evident, probably because the higher fluidity of this mixture, associated with its low viscosity, made segregation less noticeable. The presence of pigment in mixture 145P had a favorable effect compared with mixture 145R, providing greater stability and eliminating segregation, despite the increase in superplasticizer content from 0.8% to 1.0%. In mixture 155P, although the pigment reduced segregation, its effect was less pronounced, which can be explained by the low total fines content (cement and pigment) in this mixture. For the mixtures with silica fume (130S, 145S, and 155S), their effect at the 1:3.0 ratio, unlike the pigment, maintained the mixture practically free of segregation (1.35%). The same occurred for the 1:4.5 ratio, which is justified by the high specific surface area and spherical morphology of the silica fume, both of which increased viscosity and stability. At the 1:5.5 ratio, despite the reduction in segregation compared with the reference micro concrete, the segregation observed was still 9.64%. This was due to the small amount of silica in the mixture (10% replacement of cement), given the already low binder content. The presence of segregation in mixture 155S is clearly evident in Figures 3 and 4.

The combined effect of pigment and silica fume was beneficial and more pronounced compared with the reference mixtures and with the individual effects of these fines, particularly for the 1:5.5 ratio. In Figure 5b, showing mixtures 130PS, 145PS, and 155PS, the homogeneous appearance of the mixtures can be observed. For mixture 155PS, segregation was reduced by approximately 38% compared with the reference mixture 155R.

Regarding the combined effect of pigment, silica fume, and nanosilica, an even more pronounced positive effect was observed. For the 1:5.5 ratio (mixture 155PSNs), segregation was reduced by approximately 56% compared with the reference mixture 155R. The images in Figures 5 and 6, showing mixtures 130PSNs, 145PSNs, and 155PSNs, highlight cohesive mixtures without visible evidence of segregation.

Regarding the classification of NBR 15823-1 (ABNT, 2017) for segregation, all mixtures were classified as SR2 (Segregation ≤ 15%), indicating that they are suitable for critical applications, such as deep foundation elements, columns, walls, complex structural components, and prefabricated elements.

In general, it is noteworthy that systems containing silica fume, as well as those with silica fume and nanosilica (with pigment), exhibited higher viscosity—particularly apparent plastic viscosity under confined flow (V-funnel)—and lower segregation. This behavior was attributed to greater cohesion in the plastic state and increased water retention, resulting from the higher adsorption capacity of water molecules in systems with high specific surface area, as discussed previously and supported by the arguments of Cascudo, (2017). In the images of Figures 5 and 6, some evidence of segregation and increased exudation was observed in the systems containing mineral additions, compared with the reference mixtures; however, these effects were not fully confirmed in this study. The images occasionally show localized accumulation of free water at the perimeter of the "open" mixture, which was likely due to the higher dosage of superplasticizer in the mixtures containing silica fume or silica fume with nanosilica. This does not imply, however, that these mixtures were more prone to segregation or less cohesive than the reference mixtures.

4 RESULTS IN THE HARDENED STATE

The results for the mixtures in the hardened state are plotted in Figures 7 to 9. Figure 7 shows the results of compressive strength. In Figure 8, the results of the Splitting tensile strength. In Figure 9, the results of the Modulus of Elasticity at 28 days.

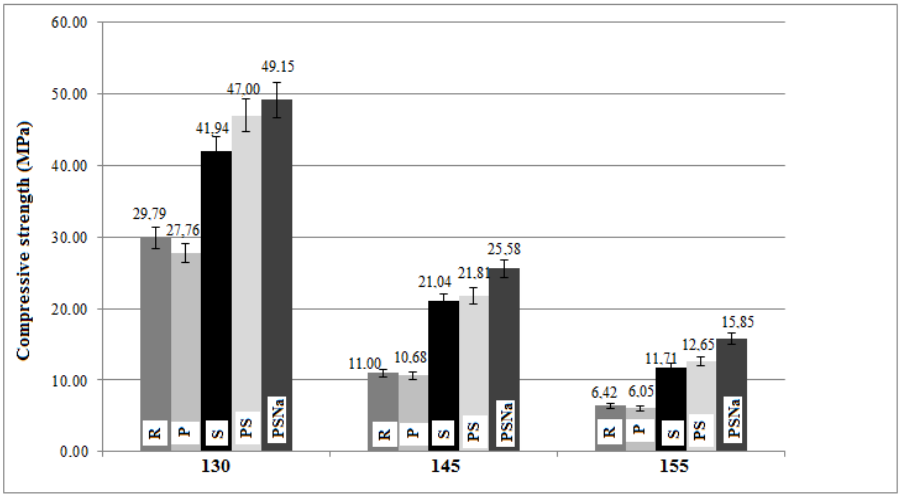

Figure 7 – Average values of compressive strength at 28 days.
Source: Author's personal catalogue (2025).

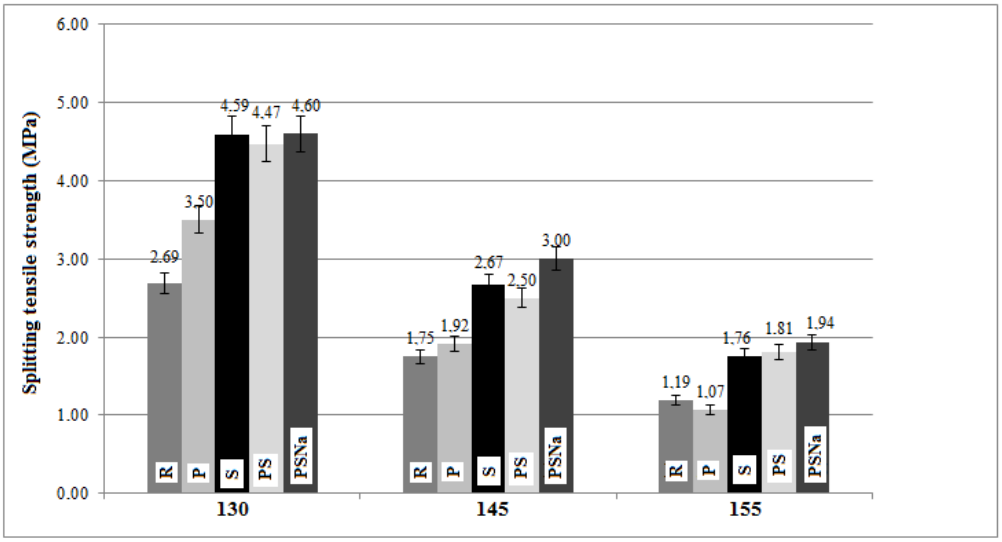

Figure 8 – Average values of splitting tensile strength at 28 days.
Source: Author's personal catalogue (2025).

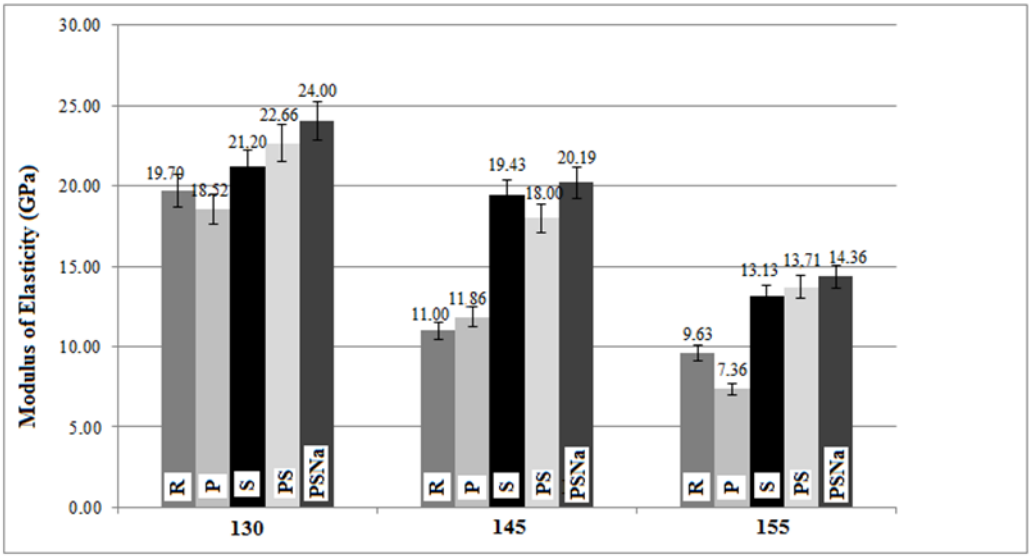

Figure 9 – Average values of the initial tangent modulus of elasticity.
Source: Author's personal catalogue (2025).

Table 7 and Table 8 present the data and the results of the statistical analysis, respectively. A discussion of these results is provided in the following subsections.

	Properties	Source	DF	SS (Aj)	MS (Aj)	Fc	Pr>Fc	Others
Mixture 130	Compressive strength	Treatment	4	1191.849627	297.962407	192.813	0.0000	*CV(%)=3.17; **Aver.: 39.21 MPa
		Repetition	2	29.376360	14.688180	9.505	0.0077	
		error	8	12.362773	1.545347			
		Total	14	1233.588760				
	Splitting tensile strength	Treatment	4	8.671800	2.167950	24.530	0.0002	CV(%)=7.49; Aver.: 3.97 MPa
		Repetition	2	0.713560	0.356780	4.037	0.0614	
		error	8	0.707040	0.088380			
		Total	14	10.092400				
	Modulus of elasticity	Treatment	4	58.208160	14.552040	11.969	0.0019	CV(%)=5.20; Aver.: 21.22 GPa;
		Repetition	2	3.877560	1.938780	1.595	0.2613	
		error	8	9.726440	1.215805			
		Total	14	71.812160				
Mixture 145	Compressive strength	Treatment	4	548.444760	137.111190	98.831	0.0000	CV(%)=6.53; Aver.: 18.04 MPa ;
		Repetition	2	14.989320	7.494660	5.402	0.0328	
		error	8	11.098680	1.387335			
		Total	14	574.532760				
	Splitting tensile strength	Treatment	4	3.272040	0.818010	27.042	0.0001	CV(%)=7.34; Aver.: 2.37 MPa
		Repetition	2	0.217000	0.108500	3.587	0.0773	
		error	8	0.242000	0.030250			
		Total	14	3.731040				
	Modulus of elasticity	Treatment	4	226.243560	56.560890	79.653	0.0000	CV(%)=5.24; Aver.: 16.10 GPa;
		Repetition	2	4.371640	2.185820	3.078	0.1020	
		error	8	5.680760	0.710095			
		Total	14	236.295960				
Mixture 155	Compressive strength	Treatment	4	213.454560	53.363640	413.575	0.0000	CV(%)=3.41; Aver.: 10.54 MPa
		Repetition	2	0.115360	0.057680	0.447	0.6546	
		error	8	1.032240	0.129030			
		Total	14	214.602160				
	Splitting tensile strength	Treatment	4	1.871160	0.467790	12.341	0.0017	CV(%)=12.53; Aver.: 1.55 MPa
		Repetition	2	0.011160	0.005580	0.147	0.8654	
		error	8	0.303240	0.037905			
		Total	14	2.185560				
	Modulus of elasticity	Treatment	4	108.785640	27.196410	25.547	0.0001	CV(%)= 8.87; Aver.: 11.64 GPa;
		Repetition	2	2.227960	1.113980	1.046	0.3947	
		error	8	8.516440	1.064555			
		Total	14	119.530040				

Where: DF = Degrees of Freedom; SS = Sum of Squares; MS = Mean Square; Fc= F-statistic; Pr = p value - CV: Coefficient of Variation; Aver = Average.

Table 7 – Results of micro concrete properties evaluated in the hardened state.
Source: Author's personal catalogue (2025).

Test	Mixture														
	130 REF	130 P	130 S	130 PS	130 PSNs	145 REF	145 P	145 S	145 PS	145 PSNs	155 REF	155 P	155 S	155 PS	155 PSNs
Compressive strength	a1	a1	a2	a3	a3	2a1	2a1	2a2	2a2	2a3	3a1	3a1	3a2	3a2	3a3
Splitting tensile strength	b1	b2	b3	b3	b3	2b1	2b1	2b2, 2b3	2b2	2b3	3b1	3b1	3b2	3b2	3b2
Modulus of elasticity	c1, c2	c1	c1, c2, c3	c2, c3	c2	2c1	2c1	2c2	2c2	2c2	3c2	3c1	3c3	3c3	3c3

Table 8 – Results of statistical significance.
Source: Author's personal catalogue (2025).

The letters a, b, and c correspond to the properties, while the number before each letter indicates the mixture and the number after the letter represents the average level. Thus, a1, a2, and a3 refer to mixture 130, compressive strength, and the three average levels: 1 for the lower, 2 for the middle, and 3 for the higher. Similarly, 3c1, 3c2, and 3c3 indicate mixture 155, modulus of elasticity, and the three average levels.

4.1 Compressive strength

Figure 7 compares the mixtures with pigments (130P, 145P, and 155P) to their respective reference mixtures (130R, 145R, and 155R). The addition of 2% colored pigment shows a tendency to reduce compressive strength. However, the statistical analysis results (Table 8) indicate no significant difference between these properties; the observed variations are random and not a function of the treatment. On the other hand, the mixtures with partial cement replacement by silica fume (130S, 145S, and 155S) show strength gains of 40.8%, 91.3%, and 82.4%, respectively, compared to their references (130R, 145R, and 155R). These gains are attributed to the well-known effects of paste densification and improvement of the material's internal structure, with particularly expressive results in the paste–aggregate transition zone due to the pozzolanic and microfiller actions of silica fume in the cement paste and at the aggregate interfaces (Cascudo *et al.*, 2014; Oliveira; Cascudo, 2018). It should be noted that these effects are more pronounced in mixtures with lower cement proportions, 145S and 155S.

The mixtures that incorporated both pigment and silica fume (130PS, 145PS, and 155PS) outperformed their respective reference mixtures (130R, 145R, and 155R), with strength gains of 57.8%,

98.3%, and 97.0%, respectively. However, the mixtures containing pigment, silica fume, and nanosilica (130PSNs, 145PSNs, and 155PSNs) achieved the highest compressive strength values overall. The combination of the siliceous fines promoted a better granular packing, with consequent densification of the cement matrix. It is important to observe, according to the results shown in Table 8, that the addition of nanosilica caused a considerable gain in the compressive strength, considering the mixtures 145PSNs, and 155PSNs (17.3% and 25.3%) in relation to mixtures with pigment and silica fume only (145PS and 155PS). This compressive strength gain was certainly a result of the pozzolanic reaction of nanosilica, and its nano-filler effect caused by particles with nanometer-scale dimensions (Madandoust *et al*., 2015). The contribution of these very fine pozzolans, especially nanosilica combined with silica fume, is undeniable in the densification of the paste and in the improvement of the interfaces with the aggregates, whose effects are substantial in terms of mechanical strength, but go beyond, also contributing to durability and in a very significant way (Oliveira; Oliveira; Cascudo, 2019).

4.2 Splitting tensile strength.

As shown in Figure 8 and Table 8, the splitting tensile strength exhibits a different behavior from the compressive strength, depending on the type of addition. This difference is attributed to the distinct loading conditions in both tests. It is observed that mixture 130P, with the addition of pigment, shows a 30.1% increase in splitting tensile strength compared to mixture 130R, without pigment. In mixtures 1:4.5 and 1:5.5, only small variations are observed in splitting tensile strength (not statistically significant) when comparing the pigment-containing (P) and reference (R) mixtures, with mixture P being slightly higher than R in the 1:4.5 proportion and slightly lower in the 1:5.5 proportion.

Regarding the 130 mixtures, the effect of pigment addition—this time favoring an increase in splitting tensile strength—can be attributed to a greater mechanical interlocking (imbrication) of particles due to the needle-like (acicular) shape of the pigment. Figures 1 and 2 illustrate the morphology of the pigment grains used. Such imbrication provides a plausible explanation for the observed increase in tensile strength. In mixtures 145 and 155, due to the lower pigment content (associated with a lower cement proportion), this interlocking effect, if present, is not perceptible.

Among the mixtures with individual additives, those containing silica fume (130S, 145S, and 155S) exhibit the best performance, resulting from the combined chemical and physical effects of the silica fume particles. Compared with the reference mixtures, strength increases of 70.6%, 52.6%, and 47.9% are observed for the 1:3.0, 1:4.5, and 1:5.5 binder-to-aggregate ratios, respectively.

Considering Table 8, the mixtures combining pigment and silica fume (130PS, 145PS, and 155PS) show similar performance levels, with only slight variations, compared to the mixtures containing silica fume alone.

For the mixtures containing pigment, silica fume, and nanosilica (130PSNa, 145PSNa, and 155PSNa), the results are comparable to those of the silica fume-only mixtures (130S, 145S, and 155S). Therefore, no additional beneficial effect is observed from the combined use of nanosilica and silica fume for this property, relative to silica fume alone.

4.3 Modulus of elasticity

Comparing Figures 9 and 7, the general trend observed in the compressive strength results is also reflected in the elastic modulus results. However, the statistical analyses presented in Table 8 reveal some differences, which are highlighted below.

Statistically, for mixtures 130 and 145, the mixtures with pigment exhibit elastic modulus values comparable to their respective reference mixtures, as shown in Table 8. In contrast, mixture 155 with pigment shows a reduction of approximately 23.6% compared to its reference mixture, unlike compressive strength, which remains at a similar level. This reduction can be attributed to the low cement content in this mixture, where the presence of pigment—an inert material with a high specific surface area—affects the concrete microstructure, increasing its deformability.

Mixtures with partial cement replacement by silica fume (145S and 155S) show increases in elastic modulus of 76.6% and 36.3%, respectively, compared to their reference mixtures (145R and 155R). Moreover, the effects of silica fume on this property are more pronounced in mixtures with lower cement content.

Mixtures combining silica fume and pigment exhibit similar behavior to those with silica fume alone when compared to the reference mixtures; the same applies to the PSNa mixtures.

Materials with higher elastic modulus, and thus greater rigidity, are those containing pozzolanic fines, particularly silica fume. More densely packed mixtures with compact interfaces clearly result in improved mechanical properties.

The contribution of silica fume is significant in increasing the elastic modulus, unlike other mineral additions such as metakaolin, which, although beneficial for mechanical strength and durability, do not substantially enhance concrete rigidity (Cascudo *et al.*, 2021).

5 CONCLUSIONS

Based on the results and discussions presented in this work, the following conclusions can be drawn:

- Regarding the isolated effects, the incorporation of pigment increases the workability of the micro concrete in the fresh state. In terms of properties in the hardened state, the addition of pigment does not cause significant changes in compressive strength, but it is effective in increasing tensile strength in mixtures with higher cement content.
- The partial replacement of cement with silica fume is beneficial. In the fresh state, it increases the cohesion of the mixtures compared to the reference mixtures, requiring a higher superplasticizer dosage. In the hardened state, it contributes to increases in compressive and splitting tensile strengths, as well as in the modulus of elasticity, particularly in mixtures with lower cement content.
- As for the combined effects, in the mixtures containing silica fume and pigment, results in hardened state were also positive, reaching compressive and tensile strength values higher than those of the reference mixtures; its performance in the hardened state was similar to micro concrete with 10% silica fume, demanding a higher content of superplasticizer.
- In the fresh state, mixtures incorporating pigment, silica fume, and nanosilica generally show reduced workability, requiring a higher superplasticizer dosage. In the hardened state, these combined mixtures exhibit higher compressive strength due to the enhanced effectiveness of pozzolanic reactions and the potentiated physical effects, such as the nanofiller action of the nanosilica particles. These effects lead these mixtures to the highest mechanical strength values, particularly in the 1:5.5 mixture.
- The yellow pigment, when used in ternary mixtures (cement and silica fume) or quaternary mixtures (cement, silica fume, and nanosilica), shows potentiated effects, thus demonstrating a synergy arising from these combined actions.

The results of this work highlight the potential of self-compacting micro concrete produced with residual sand and various mineral additions. Despite the considerable complexity of the hybrid mixtures used (ternary and quaternary blends with cement), the essential rheological requirements for self-compacting concrete applications are maintained, while the mechanical and elastic properties of the produced hybrid mixtures are enhanced. In parallel, the environmental benefit of

using crushed sand and the versatility offered by the simultaneous production of a special colored (pigmented) concrete are emphasized.

6 REFERENCES

Associação Brasileira de Normas Técnicas. *NBR 15823-1*: Concreto autoadensável - Parte 1: Classificação. Controle e recebimento no estado fresco. Rio de Janeiro: ABNT, 2017.

Associação Brasileira de Normas Técnicas. *NBR 15823-2*: Concreto autoadensável - Parte 2: Determinação do espalhamento. do tempo de escoamento e do índice de estabilidade visual - Método do cone de Abrams. Rio de Janeiro: ABNT, 2017.

Associação Brasileira de Normas Técnicas. *NBR 15823-5*: Concreto autoadensável - Parte 5: Determinação da viscosidade - Método do funil V. Rio de Janeiro: ABNT, 2017.

Associação Brasileira de Normas Técnicas. *NBR 15823-6*: Concreto autoadensável - Parte 6: Determinação da resistência à segregação - Métodos da coluna de segregação e da peneira. Rio de Janeiro: ABNT, 2017.

Associação Brasileira de Normas Técnicas. *NBR 5739*: Concreto - Ensaios de compressão de corpos de prova cilíndricos. Rio de Janeiro: ABNT, 2018.

Associação Brasileira de Normas Técnicas. *NBR 7222*: Concreto e argamassa — Determinação da resistência à tração por compressão diametral de corpos de prova cilíndricos. Rio de Janeiro: ABNT, 2011.

Associação Brasileira de Normas Técnicas. *NBR 8522-1*: Concreto endurecido – Determinação dos módulos de elasticidade e de deformação. Parte 1: Módulos estáticos à compressão. Rio de Janeiro: ABNT, 2021.

BARBOSA, M. T. G.; COURA. C. V. G; MENDES. L. O. Estudo sobre a areia artificial em substituição à natural para confecção de concreto. *Ambiente Construído*, Porto Alegre, v. 8, n. 4, p. 51-60, out/dez. 2008. Disponível em: https://seer.ufrgs.br/index.php/ambienteconstruido/article/view/5034. Acesso em: 22 out. 2025.

CAI, X.; LIU, R.; FAN, J.; LIAO, Y. The effectiveness of waste oyster shells (WOS) as a major fine aggregate replacement in concrete. *In:* INTERNATIONAL CONFERENCE ON ENERGY MATERIALS AND ENVIRONMENT ENGINEERING (ICEMEE), 7. [*s. l.*]. E3S *Web Conference*, 2021. Disponível em: https://doi.org/10.1051/e3sconf/202126102014. Acesso em: 22 set. 2025.

CAMPOS, P. E. F. Tecnologias para a construção do habitat social: o microconcreto de alto desempenho para o desenvolvimento da pré-fabricação leve. *In*: CIHEL – CONGRESSO INTERNACIONAL DA HABITAÇÃO NO ESPAÇO LUSÓFONO, 4., 2017, Covilhã.. *Anais* [...]. Covilhã: *Universidade Beira Interior,* 2017. Disponível em: http://www.habitaluso.org. Acesso em: 22 out. 2025.

CASCUDO, O. Arranjos atômicos e estrutura dos materiais. *In*: ISAIA. G. C. ed. *Materiais de Construção Civil e Princípios de Ciência e Engenharia dos Materiais*. 3. ed. rev. atual. São Paulo: Instituto Brasileiro do Concreto, 2017. v. 1. p. 172-205. (Capítulo 6). São Paulo: IBRACON, 2017. v. 1, cap. 6, p. 172-205. Disponível em: https://ibracon.org.br/publicacoes/livros_tecnicos/. Acesso em: 22 out. 2025.

CASCUDO, O.; MENDES, M. V. A. S.; CARASEK, H.; FERREIRA, R. B. Eficiência dos concretos contendo adições minerais frente à ação de cloretos. *In*: ENCONTRO LUSO-BRASILEIRO DE DEGRADAÇÃO EM ESTRUTURAS DE CONCRETO ARMADO (DEGRADA-2014), 1., 2014, Salvador. *Anais* [...]. Salvador: UFBA, 2014. Disponível em: http://www.degrada2014.org. Acesso em: 22 out. 2025.

CASCUDO, O.; PIRES. P.; CARASEK. H.; CASTRO. A.; LOPES. A. Evaluation of the pore solution of concretes with mineral additions subjected to 14 years of natural carbonation. *Cement and Concrete Composites*, Lisboa, v. 115, p. 1/103858-13, 2020. Disponível em: https://doi.org/10.1016/j.cemconcomp.2020.103858. Acesso em: 22 set. 2025.

CASCUDO, O.; TEODORO, R.; OLIVEIRA, A. M.; CARASEK. H. Effect of different metakaolins on chloride-related durability of concrete. *ACI Materials Journal*, Farmington Hills, v. 118, p. 1-12, 2021. Disponível em: http://dx.doi.org/10.14359/51732634. Acesso em: 22 set. 2025.

FELEKOĞLU, B. Effects of PSD and surface morphology of micro-aggregates on admixture requirement and mechanical performance of micro concrete. *Cement and Concrete Composites*, Lisboa, v. 29, n. 6, p. 481–489, 2007. Disponível em: https://doi.org/10.1016/j.cemconcomp.2006.12.008. Acesso em: 22 set. 2025.

FERREIRA, D. F. SISVAR: *A computer analysis system to fixed effects split plot type designs*. Revista Brasileira de Biometria, Lavras, v. 37, n. 4, p. 529-535, dec. 2019. ISSN 1983-0823. Available at: Disponível em: http://www.biometria.ufla.br/index.php/BBJ/article/view/450. Acesso em: 10 Feb. 2023.

INGALKAR, R. S.; Harle, S. M. Replacement of Natural Sand by Crushed Sand in the concrete. Replacement of Natural Sand by Crushed Sand in the Concrete. *Landscape Architecture and Regional Planning*, New York, v. 2, n. 1, p. 13-22, 2017. Disponível em: https://doi.org/10.11648/j.larp.20170201.12. Acesso em: 22 out. 2025.ISAIA, G. C.; GASTALDINI. A. L. G.; MORAES. R. Physical and pozzolanic action of mineral additions on the mechanical strength of high-performance concrete. *Cement and Concrete Composites*, Lisboa, v. 25, p. 69-76, 2003. Disponível em: https://doi.org/10.1016/S0958-9465(01)00057-9. Acesso em: 22 out. 2025.

JANG, H.; KANG, H.; SO, S. Color Expression characteristics and physical properties of colored mortar using ground granulated blast furnace slag and white Portland cement. *KSCE Journal of Civil Engineering*, Seoul, v. 18, n. 4, p. 1125-1132, 2014. Disponível em: https://doi.org/10.1007/s12205-014-0452-z. Acesso em: 22 out. 2025.

JONBI. J.; TJAHJANI A. R. I.; TINUMBIA N.; PATTINAJA. A. M.; HARYONO. B. S. Repair of rigid pavement using micro concrete material. *In*: International Conference on Rehabilitation and Maintenance in Civil Engineering. *MATEC Web of Conferences,* 4., v. 195, 2018. Disponível em: https://doi.org/10.1051/matecconf/201819501014. Acesso em: 22 out. 2025.

KADAM. S. B; SINGH. Y; LI. B. Strengthening of reinforced masonry using welded wire mesh and micro concrete - behaviour in-plain action. *Construction and Building Materials*, Oxford, v. 54, p. 247-257, 2014. Disponível em: https://doi.org/10.1016/j.conbuildmat.2013.12.033. Acesso em: 22 out. 2025.

LEE, H.-S.; LEE, J.-Y.; YU, M.-Y. Influence of iron oxide pigments on the properties of concrete interlocking blocks. *Cement and Concrete Research*, Lisboa, v. 33, 1889–1896, 2003. Disponível em: https://doi.org/10.1016/S0008-8846(03)00215-6. Acesso em: 22 out. 2025.

MADANDOUST, R.; MOHSENI, E.; MOUSAVI, S. Y.; NAMNEVIS, M. An experimental investigation on the durability of self-compacting mortar containing nano-SiO2. nano-Fe2O3 and nano-CuO. *Construction and Building Materials*, Oxford, v. 86, p. 44-50, 2015. Disponível em: https://doi.org/10.1016/j.conbuildmat.2015.03.100. Acesso em: 22 out. 2025.

MEHTA, P. K.; MONTEIRO, P. J. M. *Concreto: microestrutura. Propriedades e materiais.* Trad. HASPARYK, N. P.; HELENE, P.; PAULON, V. A. 3. ed. São Paulo. IBRACON. 2014. 674 p.

MUNDRA. S.; SINDHI. P. R; CHANDWANI. V. NAGAR. R.; AGRAWAL. V. Crushed rock sand — An economic and ecological alternative to natural sand to optimize concrete mix. *Perspectives in Science*, [*s. l.*], v. 8, p. 345-347, 2016. Disponível em: https://doi.org/10.1016/j.pisc.2016.04.070. Acesso em: 22 out. 2025.

NGUYEN, D. T.; NGUYEN, D. L.; LAM, M. N. T. An experimental investigation on the utilization of crushed sand in improving workability and mechanical resistance of concrete. *Construction and Building Materials*, Oxford, v. 326, 126766, 2022. Disponível em: https://doi.org/10.1016/j.conbuildmat.2022.126766. Acesso em: 22 out. 2025.

OERTEL, T.; HELBIG, U.; HUTTER, F.; KLETTI, H.; SEXTL, G. Influence of amorphous silica on the hydration in ultra-high performance concrete. *Cement and Concrete Research*, Lisboa, v. 58. p. 121–130, 2014. Disponível em: *https://doi.org/10.1016/j.cemconres.2014.01.006*. Acesso em: 22 out. 2025.

OLIVEIRA, A. M.; CASCUDO. O. Effect of mineral additions incorporated in concrete on thermodynamic and kinetic parameters of chloride-induced reinforcement corrosion. *Construction and Building Materials*, Oxford, v. 192, p. 467–477, 2018. Disponível em: https://doi.org/10.1016/j.conbuildmat.2018.10.100. Acesso em: 22 out. 2025.

OLIVEIRA, A. P.; OLIVEIRA. A. M.; CASCUDO. O. Influência do efeito combinado de sílica ativa e nanossílica em concretos: uma contribuição ao comportamento mecânico. *In*: CONGRESSO BRASILEIRO DO CONCRETO**,** 61.**,** 2019. Fortaleza. *Anais*.[*s. l.*]. São Paulo: IBRACON, v. 1, 2019, p. 1-16.

REZAEI-OCHBELAGH, D.; AZIMKHANI. S.; MOSAVINEJAD. H. G. Shielding and strength tests of silica fume concrete. *Annals of Nuclear Energy*, [*s. l.*], v. 45, p. 150-154, 2012. Disponível em: https://doi.org/10.1016/j.anucene.2012.02.006. Acesso em: 22 out. 2025

SILVA, R.V.; BACARJI, E.; CASCUDO, O. Mapeamento literário sobre o microconcreto. REEC – *Revista eletrônica de engenharia civil*, Goiânia, v.15, n.1, 2019. Disponível em: https://doi.org/10.5216/reec.v15i1.50421. Acesso em: 22 out. 2025.

TOKARSKI, R. B.; MATOSKI, A.; CECHIN, L.; WEBER, A.M. Comportamento das argamassas de revestimento no estado fresco, compostas com areia de britagem de rocha calcária e areia natural. *Revista Matéria*, Rio de Janeiro, v. 23, n. 3, 2018 Disponível em: https://doi.org/10.1590/S1517-707620180003.0530. Acesso em: 22 out. 2025.

TUTIKIAN, B. F.; DAL MOLIN, D.; CREMONINI, R. A practical mix design method for self-compacting concrete. *In*: CONFERENCE ON HIGH PERFORMANCE CONCRETE STRUCTURES AND MATERIALS, 5., 2008, Manaus. *Proceedings* [...].Farmington Hills, Michigan: American Concrete Institute, 2008. p. 235-250. (ACI Special Publication, 253).UYSAL, M. The use of waste maroon marble powder and iron oxide pigment in the production of coloured self-compacting concrete. *Advances in Civil Engineering*, [*s. l.*], v. 2018, art. 8093576, 2018. Disponível em: https://doi.org/10.1155/2018/8093576. Acesso em: 22 out. 2025.

VIJAYALAKSHMI, M.; SEKAR. A. S. S.; PRABHU. G. G. Strength and durability properties of concrete made with granite industry waste. *Construction and Building Materials*, Oxford, v. 46, p. 1–7, 2013. Disponível em: https://doi.org/10.1016/j.conbuildmat.2013.04.018. Acesso em: 22 out. 2025.

WONGKEO, W.; THONGSANITGARN, P.; CHAIPANICH, A. Compressive strength and drying shrinkage of fly ash-bottom ash-silica fume multi-blended cement mortars. *Materials and Design*, Oxford, v. 36**,** p. 655-662, 2012. Disponível em: https://doi.org/10.1016/j.matdes.2011.11.043. Acesso em: 22 out. 2025.

APÊNDICE – INFORMAÇÕES SOBRE O ARTIGO

CONTRIBUIÇÃO DOS AUTORES

Resumo/Abstract/Resumen: Edgar Bacarji; Andressa de Andrade Tassi; Oswaldo Cascudo; **Introdução ou Considerações iniciais:** Edgar Bacarji; Andressa de Andrade Tassi; Oswaldo Cascudo; **Referencial teórico:** Edgar Bacarji; Andressa de Andrade Tassi; Oswaldo Cascudo; **Metodologia:** Edgar Bacarji; Andressa de Andrade Tassi; Oswaldo Cascudo; **Análise de dados:** Edgar Bacarji; Andressa de Andrade Tassi; Oswaldo Cascudo; **Discussão dos resultados:** Edgar Bacarji; Andressa de Andrade Tassi; Oswaldo Cascudo; **Conclusão ou Considerações finais:** Edgar Bacarji; Andressa de Andrade Tassi; Oswaldo Cascudo; **Referências:** Edgar Bacarji; Andressa de Andrade Tassi; Oswaldo Cascudo; **Revisão do manuscrito:** Edgar Bacarji; Andressa de Andrade Tassi; Oswaldo Cascudo; **Aprovação da versão final publicada:** Edgar Bacarji; Andressa de Andrade Tassi; Oswaldo Cascudo.

CRediT - Taxonomia de Papéis de Colaborador - https://credit.niso.org/

Todos os autores contribuíram igualmente em todas as fases da produção do artigo.

As opiniões e informações expressas neste manuscrito, no que diz respeito tanto à linguagem quanto ao conteúdo, não refletem necessariamente a opinião da **Tecnia – Revista de Educação, Ciência e Tecnologia do IFG**, de seus editores e do Instituto Federal de Goiás. As opiniões são de responsabilidade exclusiva dos respectivos autores.

HISTÓRICO EDITORIAL

Submetido: 26 de fevereiro de 2025.
Aprovado: 3 de novembro de 2025.
Publicado: 30 de janeiro de 2026.

COMO CITAR O ARTIGO - ABNT

MTASSI, Andressa de Andrade; BACARJI, Edgar; MATOS, Oswaldo Cascudo. Effect of different mineral additions on colored self-compacting micro concrete produced with residual sand. Tecnia – Revista de Educação, Ciência e Tecnologia do IFG, Goiânia, v. 11, n. 1, p. 63-94, 2026.

PROCESSO DE AVALIAÇÃO

Revisão por pares duplo-cega (Double blind peer review).

AVALIADORES

Dois pareceristas ad hoc avaliaram este artigo e não autorizaram a divulgação dos seus nomes.

EDITOR(A) SEÇÃO

Prof. Dr. Marlon André Capanema
Instituto Federal de Educação, Ciência e Tecnologia de Goiás (IFG)